720–727 Nucleic Acids Research, 2000, Vol. 28, No. 3 

# Active site constraints in the hydrolysis reaction catalyzed by bacterial RNase P: analysis of precursor tRNAs with a single 3′-*S*-phosphorothiolate internucleotide linkage

**Jens M. Warnecke, Erik J. Sontheimer[1], Joseph A. Piccirilli[1] and Roland K. Hartmann***

Medizinische Universität zu Lübeck, Institut für Biochemie, Ratzeburger Allee 160, D-23538 Lübeck, Germany and [1]Howard Hughes Medical Institute, Department of Biochemistry and Molecular Biology and Department of Chemistry, University of Chicago, 5841 South Maryland Avenue, MC1028, Chicago, IL 60637, USA

Received October 7, 1999; Revised and Accepted December 3, 1999

## ABSTRACT

**Endonucleolytic processing of precursor tRNAs (ptRNAs) by RNase P yields 3′-OH and 5′-phosphate termini, and at least two metal ions are thought to be essential for catalysis. To determine if the hydrolysis reaction catalyzed by bacterial RNase P (RNAs) involves stabilization of the 3′-oxyanion leaving group by direct coordination to one of the catalytic metal ions, ptRNA substrates with single 3′-*S*-phosphorothiolate linkages at the RNase P cleavage site were synthesized. With a 3′-*S*-phosphorothiolate-modified ptRNA carrying a 7 nt 5′-flank, a complete shift of the cleavage site to the next unmodified phosphodiester in the 5′-direction was observed. Cleavage at the modified linkage was not restored in the presence of thiophilic metal ions, such as $Mn^{2+}$ or $Cd^{2+}$. To suppress aberrant cleavage, we also constructed a 3′-*S*-phosphorothiolate-modified ptRNA with a 1 nt 5′-flank. No detectable cleavage of this substrate was seen in reactions catalyzed by RNase P RNAs from *Escherichia coli* and *Bacillus subtilis*, independent of the presence of thiophilic metal ions. Ground state binding of modified ptRNAs was not impaired, suggesting that the 3′-*S*-phosphorothiolate modification specifically prevents formation of the transition state, possibly by excluding catalytic metal ions from the active site.**

## INTRODUCTION

Ribonuclease P is a ubiquitous metalloenzyme that cleaves tRNA precursor transcripts to generate the mature 5′-ends of tRNAs. Processing of precursor tRNAs (ptRNAs) by RNase P is an essentially irreversible reaction generating 3′-OH and 5′-phosphate termini. A solvent hydroxide or activated water molecule is thought to act as the nucleophile in an $S_N2$ in-line displacement mechanism (1,2). Two (3) or three (2) metal ions were proposed to mediate catalysis by bacterial RNase P RNA. The two metal ion mechanism (3), orginally proposed by Steitz and Steitz (4) for RNA-catalyzed hydrolysis and phosphoryl transfer reactions, involves direct metal ion coordination to the 3′-oxyanion leaving group in the transition state (Fig. 1). Substitution of an oxygen leaving group by sulfur provides a means to test this possibility, because different metal ions differ in their ability to coordinate oxygen versus sulfur. For example, $Mg^{2+}$ strongly resists coordination to sulfur, preferring oxygen by ~$10^4$, whereas softer cations such as $Mn^{2+}$, $Zn^{2+}$ and $Cd^{2+}$ will readily coordinate sulfur. Thus a switch in metal ion specificity upon sulfur substitution from $Mg^{2+}$ to a more thiophilic metal ion provides strong evidence that a metal ion stabilizes the leaving group by direct coordination in the transition state. This has been documented for the first and second steps of the self-splicing reactions catalyzed by the *Tetrahymena* group I intron (5,6) and by the ai5γ group II intron from *Saccharomyces cerevisiae* (7) and for the first step of pre-mRNA splicing catalyzed by the spliceosome (8). In these reactions, sulfur substitution of the leaving group has a large deleterious effect on the reaction rate in the presence of $Mg^{2+}$, but a substantial restoration of activity in the presence of thiophilic metal ions was observed, indicating that direct metal ion coordination to the leaving group occurs during catalysis.

Here we have synthesized ptRNAs with a single 3′-*S*-phosphorothiolate internucleotide linkage to investigate the proposed direct metal ion coordination to the 3′-oxyanion leaving group (Fig. 1). Modified ptRNAs were analyzed as substrates for bacterial RNase P (RNAs) under single turnover conditions (E >> S) to ensure that the rate of the chemical step was being monitored (3).

## MATERIALS AND METHODS

Synthetic oligoribonucleotides Ino (5′-CCCUUUIGCGGGA-3′), Ino-*S* [5′-CCCUUU($I_S$)GCGGGA-3′, where $I_S$ is 3′-thioinosine], Cyt (5′-CGCGGGAGUAGCUCAGUC-3′) and Cyt-*S* [5′-($C_S$)GC-GGGAGUAGCUCAGUC-3′, where $C_S$ is 3′-thiocytidine] were synthesized at the 1 µmol scale on a Millipore solid phase

*To whom correspondence should be addressed. Tel: +45 1 500 4065; Fax: +45 1 500 4068; Email: hartmann@biochem.mu-luebeck.de
Present addresses:
Jens M. Warnecke, Universität Witten/Herdecke, Institut für Molekularbiologie, Stockumer Straße 10, D-58453 Witten, Germany
Erik J. Sontheimer, Northwestern University, Department of Biochemistry, Molecular Biology and Cell Biology, 2153 North Campus Drive, Evanston, IL 60208, USA

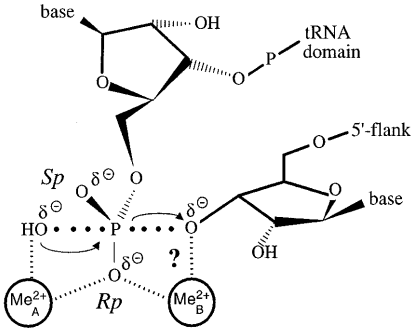


**Figure 1.** Possible mechanism for ptRNA cleavage by RNase P RNA (adapted from 3). The model includes main features of the general two metal ion mechanism proposed for protein- and RNA-catalyzed hydrolytic and phosphoryl transfer reactions (4).

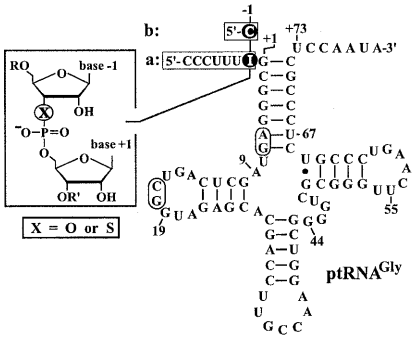


**Figure 2.** Precursor ptRNA$^{Gly}$ variants carrying a single 3′-*S*-phosphorothiolate linkage at the RNase P cleavage site. Highlighted nucleotides mark the sites of modification. Unmodified ptRNAIno and modified ptRNAIno-*S* (**a**), which carry a 7 nt 5′-flank and inosine or 3′-thioinosine at position –1, respectively, were obtained by ligation of three RNA fragments (see Materials and Methods and Results), with the sites of ligation indicated by boxes (A6/G7 and C17/G18). Unmodified and modified constructs of the type shown in (**b**) carried a 1 nt 5′-flank and were assembled from two RNA fragments (ligation between C17 and G18); natural precursor tRNA$^{Gly}$ contains a cytidine at position −1 (17). The canonical RNase P cleavage site is located between nt –1 and +1. Unmodified ptRNA$^{Gly}$, identical to ptRNAIno except for a C residue at position −1, is termed 'wild-type' ptRNA$^{Gly}$ in Table 1.

RNA/DNA synthesizer. Coupling of unmodified nucleoside phosphoramidites (Glen Research) followed standard procedures (9); synthesis and coupling of the protected cytidine 3′-*S*-phosphorothioamidite were as described by Sun *et al.* (10). Both oligonucleotides were deprotected following standard techniques (9), purified by anion exchange HPLC, further purified and desalted by reverse phase HPLC, dried *in vacuo* and resuspended in water.

### Assembly of ptRNA$^{Gly}$ variants

Assembly and ligation of ptRNA$^{Gly}$ variants was performed according to the strategies illustrated in Figure 2, essentially as described (3).

### Preparation of RNase P components

RNAs were obtained by *in vitro* run-off transcription using T7 RNA polymerase as described previously (11–13). RNase P RNA from *Bacillus subtilis* was transcribed from plasmid pDW66 (14) linearized with *Dra*I. RNase P RNA from *Escherichia coli* was transcribed from PCR templates (12) or from a pSP64 derivative encoding *E.coli* wild-type RNase P RNA (15), linearized with *Bam*HI. RNase P RNA from *Thermus thermophilus* was transcribed from plasmid pT7M1HB8 linearized with *Nar*I (16). The 3′-portion (starting at G+18) of *T.thermophilus* tRNA$^{Gly}$ was prepared by T7 transcription in the presence of 10 mM GMP, 2.5 mM GTP essentially as described (12) using a PCR template amplified from plasmid pTT675 (17). After T7 transcription, RNA preparations were digested with DNase I and then extracted with phenol:chloroform (1:1). RNAs were purified on 5–10% polyacrylamide–8 M urea gels, visualized by UV shadowing, excised from the gel and eluted overnight at 4°C in 200 mM Tris–HCl pH 7.0, 1 mM EDTA. RNAs were recovered by ethanol precipitation in the presence of 75 mM NaOAc (pH 7.0), dissolved in water and concentrations were determined by UV spectroscopy (1 $OD_{260}$ = 37 µg/ml). The *E.coli* RNase P protein was prepared as described (18).

### 5′-End-labeling of RNAs

5′-End-labeling using [γ-$^{32}$P]ATP and T4 polynucleotide kinase was performed as described (19).

### Kinetics

Single turnover experiments were performed as described (20) with trace amounts (<1 nM) of 5′-$^{32}$P-end-labeled ptRNA and 5 µM RNase P RNA in 50 mM MES, pH 6.0 or 7.0 (at 37°C), and either 1.0 M $NH_4OAc$, 15 mM divalent cations (*E.coli* RNase P RNA) or 1.0 M $NH_4OAc$, 100 mM divalent cations (*B.subtilis* RNase P RNA), unless stated otherwise. RNAs were separated on 25% polyacrylamide–8 M urea sequencing gels (in the presence of 10 mM DTT for electrophoresis of 3′-*S*-phosphorothiolate-modified RNAs) and quantified as described (20).

### Determination of apparent equilibrium dissociation constants ($K_{d\ app}$)

For measurement of apparent dissociation constants by the spin column assay (21), increasing amounts of RNase P RNA and trace amounts of radiolabeled ptRNA (<1 nM) were preincubated as described (20) in 50 mM MES, pH 6.0 (at 37°C), 0.8 or 1.0 M $NH_4OAc$, 0.05% Nonidet-P40, 0.1% SDS and 0.05 or 0.1 M $Ca(OAc)_2$. About 5–10% of the radioactivity was measured in the eluate in the absence of the ribozyme and ~65–75% eluted at high concentrations of RNase P RNA (end-point). The fraction of ptRNA in the complex was calculated as $[c.p.m._{eluate}/(c.p.m._{eluate} + c.p.m._{column})]_{[E]\ >\ 0} - [c.p.m._{eluate}/(c.p.m._{eluate} + c.p.m._{column})]_{[E]\,=\,0}$ ([E] = RNase P RNA concentration) and $K_{d\ app}$ values were determined by non-linear regression analysis as described (20).

### Nuclease P1, RNase T1 and snake venom phosphodiesterase I (SVPD) hydrolysis reactions

For limited digestion by nuclease P1, ~$10^5$ Cerenkov c.p.m. of the RNA substrate and 2.5 µg of carrier RNA were preincubated in buffer P1 (40 mM $NH_4OAc$, pH 5.3, 0.4 mM $ZnSO_4$) for 5 min at 70°C, followed by addition of 0.001–0.01 U nuclease P1 (Boehringer Mannheim) to a final reaction volume of 10 µl and

further incubation for 1 min at 70°C. For limited digestion by RNase T1, ~$10^5$ Cerenkov c.p.m. of the RNA probe and 2.5 µg of carrier RNA were incubated for 10 min at 55°C with 0.2 U RNase T1 (Pharmacia) in buffer T1 (20 mM sodium citrate, 7 M urea, 1 mM EDTA, pH 5) in a 10 µl final volume. For limited digestion by SVPD from *Crotalus adamanteus* (Boehringer Mannheim), ~$10^5$ Cerenkov c.p.m. of the RNA probe and 2.5 µg of carrier RNA were incubated for 5 min at 37°C in 10 mM $MgCl_2$, 10 mM DTT, 50 mM HEPES pH 7.5 with 0.1 or 0.2 µg SVPD in a total volume of 5 µl, unless stated otherwise. Enzymatic reactions were stopped by addition of equal volumes of gel loading buffer [2.3 M urea, 66% formamide, 10–20 mM DTT, 0.05% (w/v) each BPB and XCB in 1× TBE].

### Chemical cleavage reactions

For cleavage of 3′-*S*-phosphorothiolate linkages by $I_2$, ~$2 \times 10^4$ Cerenkov c.p.m. of the RNA probe and 2.5 µg of carrier RNA were lyophilized and dissolved in 9 µl 10 mM HEPES (pH 7.5), followed by addition of 1 µl $I_2$/EtOH (1 mg/ml $I_2$ in 20% EtOH) and incubation for 10 min at 37°C. For cleavage of 3′-*S*-phosphorothiolate linkages by $AgNO_3$, ~$2 \times 10^4$ Cerenkov c.p.m. of the RNA probe and 2.5 µg of carrier RNA were lyophilized and dissolved in 4 µl $H_2O$ (or buffer, if indicated), followed by addition of 1 µl 250 mM aqueous $AgNO_3$ solution and incubation for 30 min at 30°C. The primary reaction products are the 5′-phosphate group and the silver salt of the 3′-thiolate (22). Reaction mixtures were then diluted to 50 µl with $H_2O$ and adjusted to 5 mM DTT, and insoluble DTT–silver precipitates were removed by centrifugation (22) for 5 min in a table centrifuge at 13 000 r.p.m. (~11 000 *g*). RNAs in the supernatant were concentrated by ethanol precipitation and redissolved in gel loading buffer (see above).

## RESULTS

### Assembly of ptRNAs

Precursor tRNAs carrying a single 3′-*S*-phosphorothiolate modification at the RNase P cleavage site (Fig. 2) were synthesized by combining chemical and enzymatic RNA synthesis techniques. For construction of ptRNAIno and ptRNAIno-*S* (Fig. 2, constructs a), RNA oligonucleotides 13 nt in length, either unmodified (Ino, Fig. 3) or carrying a single 3′-*S*-phosphorothiolate modification (Ino-*S*, Fig. 3), were synthesized by phosphoramidite chemistry (see Materials and Methods). The modified or unmodified 13mer, a second 11 nt RNA oligonucleotide (obtained by either chemical or enzymatic synthesis) and a transcript representing the 3′-terminal portion of the $tRNA^{Gly}$ were annealed to a bridging DNA oligonucleotide (complementary to nt +37 to –3 of the ptRNA) for ligation by T4 DNA ligase (3; Fig. 2). For chemical synthesis reasons, the resulting ptRNA carried an inosine at position –1. The ptRNACyt and ptRNACyt-*S* (Fig. 2, constructs b) carrying a single C at the 5′-terminus (as encoded in the *T.thermophilus* $tRNA^{Gly}$ gene; 17), were constructed by ligating a modified 18mer (Cyt-*S*; see Materials and Methods) or unmodified 18mer (Cyt) to the aforementioned 3′-portion of the $tRNA^{Gly}$.

### Characterization of the 3′-*S*-phosphorothiolate linkage

Initially, the modified and unmodified 13mer RNA oligonucleotides, carrying an inosine at position 7, were characterized using chemical and enzymatic probes. Figure 3 demonstrates that the thiolate linkage is more labile to alkaline hydrolysis than normal phosphodiester bonds (lanes 1 and 2 versus 3 and 4), is susceptible to RNase T1 (lanes 5 and 6) and iodine hydrolysis (lane 7 versus 8) and relatively resistant to digestion with nuclease P1 (lane 10 versus 13). These observations are similar to those obtained for a dinucleotide containing the same modified linkage (23) and confirm that the modified 13mer RNA oligonucleotide contained a single 3′-*S*-phosphorothiolate linkage connecting nt 7 and 8. Multiple iodine cleavage products (lane 8) may represent different oxidation states of the terminal sulfur (23).

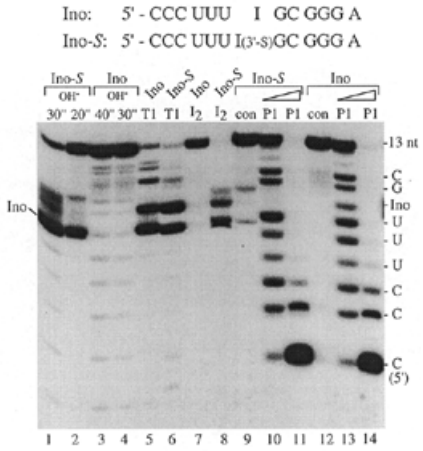


**Figure 3.** Characterization of 5′-end-labeled 13mers: Ino, unmodified 13mer; Ino-*S*, modified 13mer. Lanes 1–4, limited alkaline hydrolysis (incubation period in s); lanes 5 and 6, limited digestion by nuclease T1; lanes 7 and 8, iodine hydrolysis; lanes 10, 11, 13 and 14, limited digestion (1 min at 70°C) with nuclease P1 (lanes 10 and 13, 0.001 U; lanes 11 and 14, 0.01 U); lanes 9 and 12, control lanes in the absence of nuclease P1. Assignment of nucleotides to P1 hydrolysis bands is shown in the right margin; products corresponding to alkaline hydrolysis and RNase T1 cleavage at the 3′-side of the inosine residue at position 7 are indicated on the left. Note that alkaline hydrolysis and RNase T1 cleavage generates 3′-phosphate termini, whereas nuclease P1 cleavage products carry 3′-OH termini. Hydrolysis products were analyzed on 25% polyacrylamide–8 M urea sequencing gels in the presence of 10 mM DTT (for further details see Materials and Methods).

### Cleavage site selection

We analyzed the 5′-cleavage products generated by *E.coli* RNase P RNA-catalyzed processing of ptRNAIno and ptRNAIno-*S*. Representative results are illustrated in Figure 4. Processing of the unmodified ptRNAIno by *E.coli* RNase P RNA in the presence of $Mg^{2+}$ (Fig. 4b, lane 14) or $Mn^{2+}$ (Fig. 4c, lane 1 or 6) resulted predominantly in the expected 7 nt 5′-cleavage product. A low extent of aberrant cleavage occurred at position –2/–1 (~5% in the presence of 15 mM $Mg^{2+}$ or $Mn^{2+}$), yielding a 6 nt 5′-cleavage product, which can be attributed to formation of an $I_{-1}$:$U_{+73}$ base pair. It has been shown that the stability of the –1/+73 base pair is correlated with the propensity of *E.coli* RNase P RNA to cleave at the aberrant –2/–1 site (24,25). Processing of the 3′-*S*-phosphorothiolate-modified ptRNAIno-*S* under various conditions, some of which are shown in Figure 4 (a, lanes 4–7; b, lanes 11–13, 15 and 16) resulted exclusively in a 5′-cleavage product that migrated at the position of a 6 nt RNA fragment, suggesting aberrant cleavage between positions –2 and –1 (Fig. 2). This conclusion is supported by

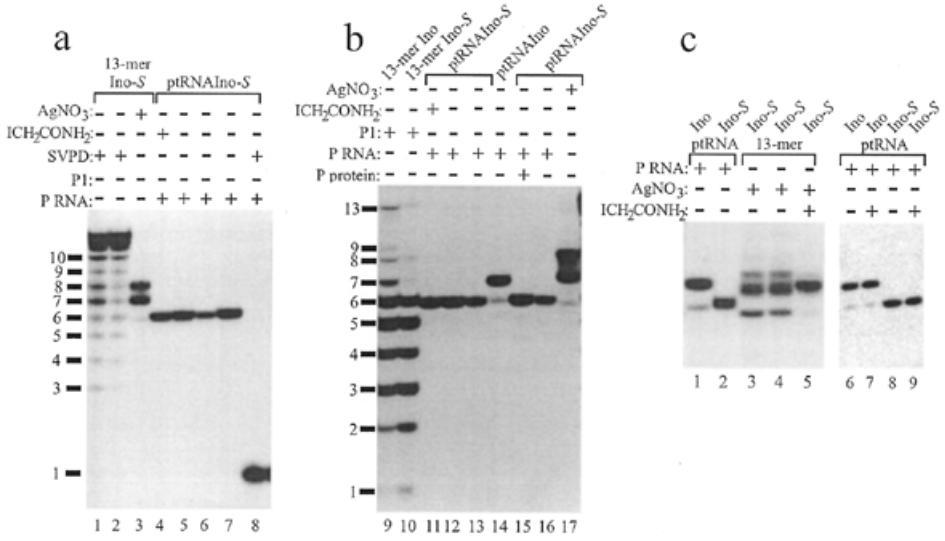


**Figure 4.** Analysis of 5′-cleavage products derived from RNase P (RNA)-catalyzed cleavage of 5′-end-labeled control ptRNAIno and ptRNAIno-*S*. (**a**) Lanes 1 and 2, limited digestion of 13mer Ino-*S* with 0.2 (lane 1) or 0.1 µg/5 µl (lane 2) SVPD; lane 3, $AgNO_3$ cleavage of 13mer Ino-*S* under RNase P RNA processing conditions [1 M $NH_4OAc$, 15 mM $Mg(OAc)_2$, pH 6.0]; lane 7, 5′-cleavage products derived from processing of ptRNAIno-*S* (<1 nM) by *E.coli* RNase P RNA (P RNA, 5 µM) under conditions of 1 M $NH_4OAc$, 15 mM $Mn(OAc)_2$, pH 6.0; lanes 4 and 5, as lane 7, but in the presence of 40 mM $ICH_2C(O)NH_2$ (lane 4) or 10 mM DTT (lane 5); lane 6, as lane 7, but using chloride instead of acetate salts; lane 8, [5′-$^{32}$P]CMP obtained by RNase P RNA cleavage as in lane 7 and additional treatment of the 5′-cleavage product with 0.3 mU SVPD. (**b**) Lanes 9 and 10, limited digestion of 13mer Ino (lane 9) and 13mer Ino-*S* (lane 10) with 0.005 U of nuclease P1. Lanes 11–13, identical to lanes 4–6 of (a); lanes 14 and 16, processing of ptRNAIno (lane 14) or ptRNAIno-*S* (lane 16) by *E.coli* RNase P RNA in the presence of 1 M $NH_4OAc$, 15 mM $Mg(OAc)_2$, pH 6.0; lane 15, processing of ptRNAIno-*S* in the presence of 1 µM *E.coli* RNase P RNA and 2 µM *E.coli* RNase P protein C5 under conditions of 10 mM $Mg(OAc)_2$, 0.1 M $NH_4OAc$, 50 mM MES–acetate, pH 7.0; lane 17, 3′-*S*-phosphorothiolate-specific cleavage of ptRNAIno-*S* by $AgNO_3$ in RNase P RNA cleavage buffer [1 M $NH_4OAc$, 15 mM $Mg(OAc)_2$, pH 6.0]. (**c**) Derivatization of free thiol groups by $ICH_2C(O)NH_2$. Lanes 1 and 2, 5′-cleavage products derived from processing of <1 nM ptRNAIno (lane 1) or ptRNAIno-*S* (lane 2) by *E.coli* RNase P RNA (5 µM) under conditions of 1 M $NH_4OAc$, 15 mM $Mn(OAc)_2$, pH 6.0; lane 3, $AgNO_3$ hydrolysis of 13mer Ino-*S* in $H_2O$; lanes 4 and 5, as lane 3, but additional incubation in 80 mM HEPES pH 7.5 (lane 4) or 80 mM HEPES pH 7.5, plus 50 mM $ICH_2C(O)NH_2$ (lane 5). Lanes 6–9, RNase P RNA processing of ptRNAIno (lanes 6 and 7) or ptRNAIno-*S* (lanes 8 and 9) as in lanes 1 and 2, respectively, followed by removal of salts by ethanol precipitation and washing of the precipitate with 70% EtOH, resolving of the pellet in $H_2O$ (lanes 6 and 8) or additional treatment with 40 mM $ICH_2C(O)NH_2$ in 50 mM HEPES pH 7.5 (lanes 7 and 9). Hydrolysis products were analyzed on 25% polyacrylamide–8 M urea sequencing gels in the presence of 10 mM DTT (for further details see Materials and Methods).

the absence of changes in gel mobility when the thiol-modifying reagent $ICH_2C(O)NH_2$ was present during RNase P processing (Fig. 4a, lane 4, and b, lane 11), when processing was performed under reducing conditions (10 mM DTT; Fig. 4a, lane 5, and b, lane 12) or when the acetate salts of the processing buffer were replaced by chloride salts (Fig. 4a, lane 6, and b, lane 13). The *E.coli* RNase P holoenzyme also produced the shorter 5′-cleavage product (Fig. 4b, lane 15). Finally, neither the presence of more thiophilic divalent metal ions ($Mn^{2+}$, $Cd^{2+}$, $Zn^{2+}$ or $Co^{2+}$) nor the use of other RNase P RNAs (e.g. from *B.subtilis* or *T.thermophilus*) changed the observed cleavage site selection for ptRNAIno-*S* (data not shown).

To further substantiate our conclusion that the 3′-*S*-phosphorothiolate modification prevented RNase P-catalyzed processing at the canonical cleavage site, we performed a limited digestion of the 13mer Ino-*S* (used for the assembly of ptRNAIno-*S*; Fig. 2) by SVPD, which, like RNase P, generates 5′-phosphate termini and efficiently hydrolyzes 3′-*S*-phosphorothiolate linkages (22). As shown in Figure 4a (lanes 1 and 2), the 7 nt fragment carrying a 3′-thiol group showed no significant deviation in gel mobility under the electrophoresis conditions applied, although the sulfur is expected to be deprotonated and therefore to carry an extra negative charge compared with a 3′-OH group (10,23). 3′-*S*-phosphorothiolate-specific hydrolysis of 13mer Ino-*S* or ptRNAIno-*S* by $AgNO_3$, which also yields 3′-SH termini (23), resulted in two main cleavage products under RNase P processing conditions that showed reduced gel mobility compared with the RNase P RNA cleavage product of ptRNAIno-*S* (Fig. 4a, lane 3, and b, lane 17). It is unclear why more than one band results from $AgNO_3$-catalyzed hydrolysis; this may reflect different oxidation states of the terminal sulfur, similar to the multiple oxidation states observed after iodine cleavage of 3′-*S*-phosphorothiolate linkages (22). We next analyzed the susceptibility of RNase P RNA- and $AgNO_3$-generated hydrolysis products to derivatization by iodoacetamide [$ICH_2C(O)NH_2$; Fig. 4c]. As demonstrated in lane 5, we were able to derivatize $AgNO_3$ hydrolysis products, resulting in a single product band that migrated at the same position as the unmodified 7 nt 5′-flank generated by RNase P cleavage of unmodified ptRNAIno (lane 1). This is consistent with the observation that an unmodified 8 nt RNA oligonucleotide showed nearly the same gel mobility under similar electrophoresis conditions as an 8 nt RNA fragment carrying a 3′-terminal sulfur derivatized by iodoacetamide (7). Unlike the $AgNO_3$ hydrolysis products, the 5′-cleavage product derived from RNase P RNA processing of ptRNAIno-*S* remained unaffected by incubation with $ICH_2C(O)NH_2$ (Fig. 4c, lane 9), migrating faster than $ICH_2C(O)NH_2$-derivatized $AgNO_3$ hydrolysis products (lane 5).

In summary, the data presented in Figures 3 and 4 indicate that the 13mer Ino-*S* and ptRNAIno-*S* carried a single 3′-*S*-phosphorothiolate modification at the RNase P cleavage site and that this modification prevents cleavage by bacterial RNase P (RNA), resulting in a complete shift of the cleavage site to the next unmodified phosphodiester in the 5′-direction under the various conditions tested.

## Single turnover kinetics

Single turnover experiments with ptRNAIno-*S* and the control substrate ptRNAIno were performed with trace amounts (<1 nM) of 5′-$^{32}$P-end-labeled ptRNAs and 5 µM *E.coli* RNase P RNA in the presence of 1 M $NH_4OAc$ at pH 6.0. Metal ion-dependent cleavage rates ($k_{obs}$) are summarized in Table 1. The rates for cleavage of the unmodified ptRNAIno were in the range 0.2–0.5 min$^{-1}$ in the presence of $Mg^{2+}$ and/or $Mn^{2+}$, ~3- to 7-fold slower than the rate observed for the normal ptRNA$^{Gly}$ carrying the same 7 nt 5′-flank but a C at position –1 (3). This suggests that a purine at position –1 somewhat reduces cleavage efficiency of ptRNA$^{Gly}$ by *E.coli* RNase P RNA. Processing of ptRNAIno-*S* at the aberrant cleavage site (position –2/–1) was less efficient, but occurred at a 10-fold higher rate in the presence of $Mn^{2+}$ compared with $Mg^{2+}$. The dependence of cleavage efficiency and cleavage site selection by *E.coli* RNase P RNA on metal ion identity has previously been described for other ptRNA substrates (24).

**Table 1.** Cleavage of ptRNAIno, ptRNAIno-*S* and 'wild-type' ptRNA$^{Gly}$ by *E.coli* RNase P RNA[a]

| ptRNA species | Metal ions | $k_{obs}$ (min$^{-1}$) |
|---|---|---|
| ptRNAIno | 15 mM $Mg^{2+}$ | 0.46 ± 0.1 (0.023)[b] |
| | 12.5 mM $Mg^{2+}$, 2.5 mM$Mn^{2+}$ | 0.21 ± 0.02 |
| | 15 mM $Mn^{2+}$ | 0.23 ± 0.07 (0.012)[b] |
| ptRNAIno-*S* | 15 mM $Mg^{2+}$ | 0.015 ± 0.01 |
| (cleavage at nt –2/–1) | 15 mM $Mg^{2+}$, 2.5 mM $Mn^{2+}$ | 0.04 |
| | 15 mM $Mn^{2+}$ | 0.16 ± 0.01 |
| ptRNA$^{Gly}$ | 15 mM $Mg^{2+}$ | 3.3 ± 1.0 |
| (cleavage at nt –1/+1)[c] | 12.5 mM $Mg^{2+}$, 2.5 mM$Mn^{2+}$ | 1.5 ± 0.4 |
| | 15 mM $Mn^{2+}$ | 0.75 ± 0.25 |

[a]$k_{obs}$ values for ptRNAIno and ptRNAIno-*S* represent mean values of two independent experiments and errors indicate deviations between individual experiments.

[b]Cleavage at position –2/–1 in parentheses estimated as follows (33):

$$k_{obs} = k_{obs}^{(-1/+1)} + k_{obs}^{(-2/-1)} \quad \mathbf{1}$$

and

$$k_{obs}^{(-2/-1)} = [\text{c.p.m. } P(-2/-1)_t / \{\text{c.p.m. } P(-2/-1)_t + \text{c.p.m. } P(-1/+1)_t\}] \times k_{obs} \quad \mathbf{2}$$

with $P$ = product, $t$ = time, (–2/–1) = aberrant cleavage site and (–1/+1) = normal cleavage site, and based on ~5% cleavage at position –2/–1 in the presence of 15 mM $Mg^{2+}$ or $Mn^{2+}$. Assuming that $k_{obs} \approx k_{obs}^{(-1/+1)}$ and $k_{obs}$ = 0.23 min$^{-1}$ at 15 mM $Mn^{2+}$, it follows from equation **2** that $k_{obs}^{(-2/-1)} = 0.05 \times 0.23$ min$^{-1}$ = 0.012 min$^{-1}$.

[c]Taken from Warnecke *et al.* (3).

## Construction and analysis of modified ptRNA with a 1 nt 5′-flank

Our results obtained with ptRNAIno-*S* did not exclude the possibility that slow cleavage at the modified canonical site was masked by relatively fast cleavage at position –2/–1. Use of a ptRNA with a 1 nt 5′-flank would exclude a shift of the cleavage site to the –2/–1 position and may permit analysis of slow processing at the modified site. Towards this goal, we first investigated processing of unmodified ptRNACyt by *E.coli* RNase P RNA to make sure that the 1 nt flank is removed with reasonable efficiency and that no cleavage occurs at position +1/+2. Processing exclusively resulted in formation of the 1 nt 5′-cleavage product, as confirmed by co-electrophoresis with the radiolabeled dinucleotide pCpG (data not shown). The single turnover rate of cleavage was determined to be ~0.2 min$^{-1}$ (<1 nM ptRNACyt, 4 µM *E.coli* RNase P RNA, 1 M $NH_4OAc$ and 15 mM $Mg^{2+}$, pH 6.0). This rate is 2.3-fold lower than that measured for ptRNAIno under very similar conditions (Table 1). It seems that the favorable effect of a C at position –1 (see above) in ptRNACyt is counteracted by the presence of a 1 nt 5′-flank compared with a 7 nt 5′-flank in ptRNAIno. Kinetic experiments with *B.subtilis* RNase P indeed provided evidence that substrate affinity and the cleavage rate constant may decrease for a ptRNA with a 1 nt 5′-flank relative to substrates with longer 5′-precursor segments (26). We then constructed ptRNACyt-*S*, carrying the same 1 nt 5′-flank and a single 3′-*S*-phosphorothiolate linkage at the RNase P cleavage site (Fig. 2b). The presence of the modified linkage was verified by iodine hydrolysis, $AgNO_3$ hydrolysis and derivatization of the $AgNO_3$ hydrolysis product by $ICH_2C(O)NH_2$ (data not shown). We then analyzed processing of ptRNACyt and ptRNACyt-*S* by *E.coli* RNase P RNA under standard single turnover conditions in the presence of either 15 mM $Mg^{2+}$ or $Mn^{2+}$. No significant processing within 3 h occurred in the case of ptRNACyt-*S* under either condition (Fig. 5a, lanes 4–6 and 10–12), as inferred from the fact that we were unable to observe any loss of 5′-end-label from the substrate over this period. In contrast, processing of ptRNACyt was almost complete after 10 min (lanes 1–3 and 7–9).

We have previously shown that cleavage of a ptRNA with a single $R_p$-phosphorothioate modification by *E.coli* RNase P RNA is most efficiently restored in the presence of $Cd^{2+}$ (3). However, the presence of $Cd^{2+}$ did not restore processing of ptRNACyt-*S* to any significant extent (Fig. 5b). The 5′-end-label remained entirely on the substrate or, in some experiments and after prolonged incubation periods, formation of aberrant high molecular weight products due to cleavage somewhere in the 3′-portion of the mature tRNA moiety was observed (Fig. 5b; see the 21 h time point in the simultaneous presence of $Mg^{2+}$ and $Cd^{2+}$). However, we were unable to detect accumulation of a low molecular weight cleavage product that could have corresponded to the $pC_{SH}$ mononucleotide in any of our experiments. This holds true for a variety of additional reaction conditions tested, such as pH 7.0 instead of 6.0 and elevated metal ion concentrations (100 mM $Mg^{2+}$, 100 mM $Mn^{2+}$, 80 mM $Mg^{2+}$ + 20 mM $Cd^{2+}$, $Zn^{2+}$ or $Co^{2+}$). In contrast, unmodified ptRNACyt was efficiently converted to mature tRNA under all of these conditions (data not shown).

We also tested processing of ptRNACyt and ptRNACyt-*S* by *B.subtilis* RNase P RNA in the presence of different metal ions and metal ion combinations (Fig. 5c). Since processing reactions were performed in the presence of $ICH_2C(O)NH_2$, which did not interfere with RNase P activity (Fig. 4a and b, lanes 4 and 11, respectively), we expected a 5′-cleavage product of ptRNACyt-*S* to co-migrate with the iodoacetamide derivative

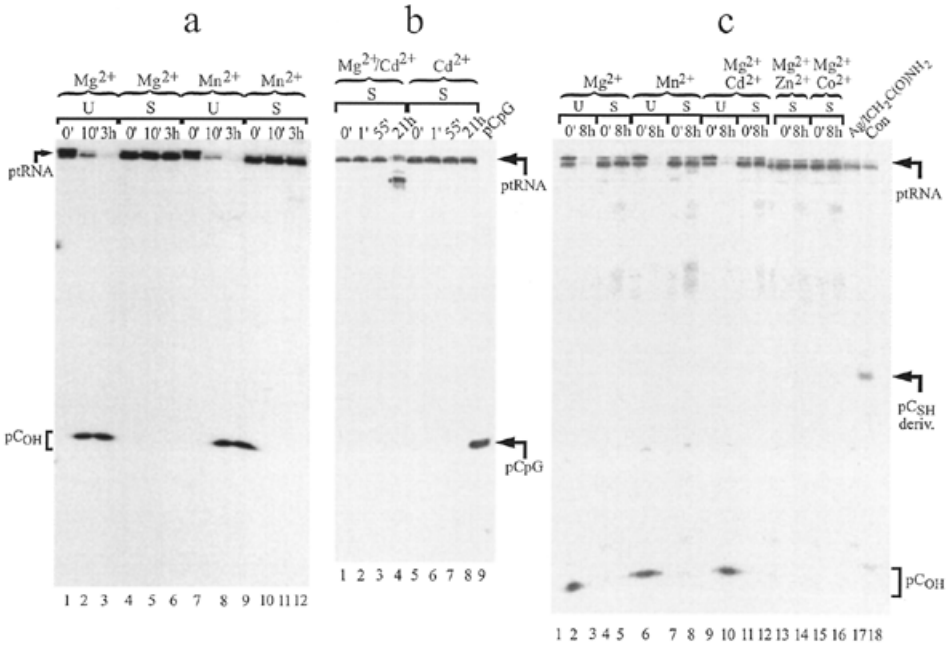


**Figure 5.** Processing of <1 nM 5′-end-labeled ptRNACyt (U) or ptRNACyt-*S* (S) in the presence of 5 µM (**a** and **b**) *E.coli* or (**c**) *B.subtilis* RNase P RNA at 37°C. Aliquots were withdrawn at indicated time points and analyzed on 25% polyacrylamide–8 M urea sequencing gels in the presence of 10 mM DTT. (a) Reaction conditions: 1 M $NH_4OAc$, pH 6.0, and either 15 mM $Mg(OAc)_2$ or 15 mM $Mn(OAc)_2$. (b) Reaction conditions: 1 M $NH_4OAc$, pH 6.0, and either 12.5 mM $Mg(OAc)_2$/2.5 mM $Cd(OAc)_2$ or 15 mM $Cd(OAc)_2$. [5′-$^{32}$P]pCpG (outer lane on the right) served as a size standard. Two imaging plates were required for analysis of this gel, resulting in a small gap within lane 4. (c) Reaction conditions: 1 M $NH_4OAc$, 40 mM $ICH_2C(O)NH_2$, pH 7.0, and either 100 mM $Mg(OAc)_2$, 100 mM $Mn(OAc)_2$, 80 mM $Mg(OAc)_2$/20 mM $Cd(OAc)_2$, 80 mM $Mg(OAc)_2$/20 mM $Zn(OAc)_2$ or 80 mM $Mg(OAc)_2$/20 mM $Co(OAc)_2$. Lane Ag/$ICH_2C(O)NH_2$, incubation of ptRNACyt-*S* in the presence of 1 M $NH_4OAc$, 15 mM $Mg(OAc)_2$, pH 7.0, 50 mM $AgNO_3$ and 40 mM $ICH_2C(O)NH_2$ for 30 min at 30°C. The indicated iodoacetamide derivative (pC$_{SH}$ deriv.) has a lower gel mobility than pC$_{OH}$, consistent with previous observations (23). Lane Con, untreated ptRNACyt-*S*. Note that products in lane Ag/$ICH_2C(O)NH_2$ merged into the outer lane (lane Con). Two imaging plates were required for analysis of this gel, resulting in a small gap within lane 12.

of pC$_{SH}$ in lane Ag/$ICH_2C(O)NH_2$. However, neither significant accumulation of such a cleavage product nor of any other product suggestive of RNase P RNA processing was observed.

### Binding of ptRNACyt and ptRNACyt-*S* to RNase P RNAs

In a previous study we have observed that an $S_p$-phosphorothiote modification at the RNase P cleavage site reduced the affinity of ptRNA ground state binding to *E.coli* RNase P RNA ~30-fold (3). Here we analyzed ground state binding of ptRNACyt and ptRNACyt-*S* to RNase P RNAs from *E.coli* and *B.subtilis* using the gel filtration centrifuge column assay (21). Binding to *E.coli* RNase P RNA was assayed under conditions of 1 M $NH_4OAc$, 0.05 M $Ca(OAc)_2$, pH 6.0, and binding to *B.subtilis* RNase P RNA in 0.8 M $NH_4OAc$, 0.1 M $Ca(OAc)_2$, pH 6.0. $Ca^{2+}$ promotes binding to RNase P RNA with similar efficiency to $Mg^{2+}$ (2,12), but essentially abolishes cleavage by RNase P RNA at pH 6.0 (2,27). Apparent $K_d$ values for the binding of ptRNACyt and ptRNACyt-*S* to *E.coli* and *B.subtilis* RNase P RNA were in the range 1–10 nM (data not shown), indicating that the 3′-*S*-phosphorothiolate modification had no significant effect on substrate binding in the presence of $Ca^{2+}$. Assuming that this also holds for enzyme–substrate ground state binding in the presence of $Mg^{2+}$ or $Mn^{2+}$, the defect caused by the sulfur modification seems to be in subsequent catalytic steps.

## DISCUSSION

Two ptRNA variants carrying a 3′-*S*-phosphorothiolate modification at the canonical RNase P cleavage site were subjected to processing by bacterial RNase P (RNAs). In the context of ptRNAIno-*S* carrying a 7 nt 5′-flank, the sulfur substitution prevented cleavage of the modified phosphodiester by bacterial RNase P activities and directed cleavage to the next unmodified phosphodiester in the 5′-direction. This was observed with different bacterial RNase P RNAs and with the *E.coli* RNase P holoenzyme and was independent of the absence or presence of thiophilic metal ions. Our experimental results do not reveal the molecular nature of the observed inhibition effects, although metal ion exclusion is one possible explanation (as discussed below). In addition, several chemical and structural differences introduced by the sulfur modification may have contributed to the loss of catalytic function. In general, substitution of sulfur for bridging or non-bridging phosphate oxygens may lead to steric effects due to the larger van der Waals radius of sulfur versus oxygen and/or to somewhat different angles and lengths of P–S and S–C bonds. Also, sulfur has a lower electronegativity and has a lower propensity to donate electron density into the phosphorus *d* orbitals than oxygen (28). As described above, sulfur has a higher affinity for transition metal ions (such as $Mn^{2+}$, $Zn^{2+}$ and $Cd^{2+}$) compared with alkaline earth ions such as $Mg^{2+}$ (29–31).

In the hydrolysis reactions catalyzed by *E.coli* RNase P (RNA) (3,32) as well as *B.subtilis* RNase P RNA (20), we have now observed the following effects of sulfur substitutions at the scissile phosphodiester. (i) Under rate limiting chemistry, an $R_p$-phosphorothioate modification is cleaved in the presence of $Mg^{2+}$ only, although at a ≥1000-fold decreased rate; $Mn^{2+}$, and particularly $Cd^{2+}$, largely restore the rate of cleavage, indicating direct metal ion coordination to the (*pro*)-$R_p$ substituent at the cleavage site (3). An (ii) $S_p$-phosphorothioate or (iii) 3′-*S*-phosphorothiolate modification essentially abolishes cleavage at the modified internucleotide linkage, even in the presence of thiophilic metal ions, and directs cleavage to the next unmodified phosphodiester in the 5′-direction (3,20; this study). As mentioned in Results, ptRNAIno was cleaved to ~5% at position –2/–1 in the presence of 15 mM $Mg^{2+}$ or $Mn^{2+}$, corresponding to a rate of ~0.02 $min^{-1}$ at 15 mM $Mg^{2+}$ and ~0.01 $min^{-1}$ at 15 mM $Mn^{2+}$ (Table 1; 33). In comparison, ptRNAIno-*S* was cleaved at position –2/–1 at a rate of 0.015 $min^{-1}$ at 15 mM $Mg^{2+}$ and 0.16 $min^{-1}$ at 15 mM $Mn^{2+}$ (Table 1). This suggests that the rate of cleavage at –2/–1 is accelerated at least 10-fold in the presence of the 3′-*S*-phosphorothiolate modification with $Mn^{2+}$, but not with $Mg^{2+}$.

Recently, it has been shown for the crystal structure of an $S_p$-phosphorothioate-modified substrate bound to the 3′→5′ exonucleolytic active site of the large fragment of DNA polymerase I from *E.coli* that the bulky sulfur atom displaces essential catalytic metal ions from the active site (34). Analogously, the $S_p$-phosphorothioate and 3′-*S*-phosphorothiolate modifications could lead to exclusion of metal ion(s) from the active site of bacterial RNase P (RNA)–substrate complexes, possibly because of the bulkiness of the sulfur atom or because the sulfur substitution prevents correct positioning of the scissile bond in the active site. Recent X-ray analyses of a heptamer deoxynucleotide containing a single 3′-*S*-phoshorothiolate linkage bound to the 3′→5′ exonucleolytic active site of *E.coli* DNA polymerase I in the presence of different metal ions ($Mg^{2+}$, $Mn^{2+}$ or $Zn^{2+}$) or combinations thereof have revealed little effect of the sulfur modification on positioning of the DNA in the active site (31). However, the sulfur substitution abolished binding of $Mg^{2+}$ to metal ion site B (corresponding to metal ion site B in Fig. 1), whereas $Mn^{2+}$ and $Zn^{2+}$ were still able to bind this site. Although $Mn^{2+}$ was able to occupy metal ion site B in the presence of the 3′-*S*-phoshorothiolate modification, exonuclease activity was ~600-fold reduced for the modified versus the all-oxygen substrate in the presence of $Mn^{2+}$ (31,35). Thus, in the presence of a sulfur modification, thiophilic metal ions such as $Mn^{2+}$, though able to accept sulfur as a ligand, could still be positioned in a manner that is suboptimal for stabilization of the transition state. It should also be noted that the 3′→5′ exonuclease of *E.coli* DNA polymerase I is much more efficient at cleaving all-oxygen, single-stranded DNA substrates in the presence of $Mn^{2+}$ than in the presence of $Mg^{2+}$ (31,35), which is not the case for RNase P cleavage at the canonical site (Table 1; 3). It is conceivable that the aforementioned 600-fold reduction effect in the exonuclease system may be exceeded in other systems, such as the RNase P hydrolysis reaction. This may reduce the cleavage activity below the limit of detection, particularly when the enzyme catalyzes cleavage of the natural all-oxygen substrates less efficiently with $Mn^{2+}$ than with $Mg^{2+}$. Thus, failure to observe a rescue of processing of the 3′-*S*-phosphorothiolate-modified substrate in the presence of thiophilic metal ions does not preclude the possibility that the 3′-bridging oxygen is part of the coordination sphere of catalytic metal ions in RNase P (RNA)–substrate complexes.

Our experimental observations reveal some mechanistic resemblance to the hydrolytic spliced exon reopening (SER) reaction catalyzed by self-splicing group II introns (7,36). The SER reaction is, by the criterion of stereospecificity, analogous to the reverse of step two of group II intron splicing (36). Podar *et al.* (36) have shown that the SER reaction proceeds in the presence of an $R_p$-phosphorothioate modification at the exon–exon junction, whereas hydrolysis is essentially abolished in the presence of an $S_p$-phosphorothioate modification. Very similar to the bacterial RNase P system, $S_p$-diastereomeric group II intron substrates were cleaved with low efficiency at neighboring unmodified linkages. Likewise, essentially no cleavage at the canonical exon–exon junction was observed in the SER reaction when the 3′-bridging oxygen was replaced with sulfur (7). Again, aberrant cleavage occurred at neighboring unmodified phosphodiester bonds. A difference between the group II intron-catalyzed SER reaction and the reaction catalyzed by bacterial RNase P RNA is the absence of an obvious inhibition effect due to the $R_p$ modification in the SER hydrolysis reaction (36). There is, however, the formal possibility that the SER reaction was not studied under conditions of rate limiting chemistry, which may have masked a potential $R_p$-phosphorothioate inhibition effect, as recently documented for an $S_p$-phosphorothioate modification in the first step of group II intron-catalyzed splicing (37). In conclusion, the above-mentioned similarities between the hydrolytic SER reaction catalyzed by group II self-splicing introns and the hydrolysis reaction catalyzed by bacterial RNase P RNA provide evidence that the two reactions are mechanistically related.

## ACKNOWLEDGEMENTS

We are grateful to Sengen Sun for the synthesis of RNA oligonucleotides and Rita Held for technical assistance. Financial support for these studies from the Deutsche Forschungsgemeinschaft (Ha 1672/7-1/7-2/4-2/4-3) is acknowledged.

## REFERENCES

1. Guerrier-Takada,C., Haydock,K., Allen,L. and Altman,S. (1986) *Biochemistry*, **25**, 1509–1515.
2. Smith,D. and Pace,N.R. (1993) *Biochemistry*, **32**, 5273–5281.
3. Warnecke,J.M., Fürste,J.P., Hardt,W.-D., Erdmann,V.A. and Hartmann,R.K. (1996) *Proc. Natl Acad. Sci. USA*, **93**, 8924–8928.
4. Steitz,T.A. and Steitz,J.A. (1993) *Proc. Natl Acad. Sci. USA*, **90**, 6498–6502.
5. Piccirilli,J.A., Vyle,J.S., Caruthers,M.H. and Cech,T.R. (1993) *Nature*, **361**, 85–88.
6. Weinstein,L.B., Jones,B.C.N.M., Cosstick,R. and Cech,T.R. (1997) *Nature*, **388**, 805–808.
7. Sontheimer,E.J., Gordon,P.M. and Piccirilli,J.A. (1999) *Genes Dev.*, **13**, 1729–1741.
8. Sontheimer,E.J., Sun,S. and Piccirilli,J.A. (1997) *Nature*, **388**, 801–805.
9. Gait,M.J., Pritchard,C. and Slim,G. (1991) In Eckstein,F. (ed.), *Oligonucleotides and Analogs: A Practical Approach*. Oxford University Press, Oxford, UK, pp. 25–48.
10. Sun,S., Yoshida,A. and Piccirilli,J.A. (1997) *RNA*, **3**, 1352–1363.
11. Schlegl,J., Fürste,J.P., Bald,R., Erdmann,V.A. and Hartmann,R.K. (1992) *Nucleic Acids Res.*, **20**, 5963–5970.
12. Hardt,W.-D., Schlegl,J., Erdmann,V.A. and Hartmann,R.K. (1993) *Nucleic Acids Res.*, **21**, 3521–3527.

13. Hardt,W.-D., Erdmann,V.A. and Hartmann,R.K. (1996) *RNA*, **2**, 1189–1198.
14. Smith,D., Burgin,A.B., Haas,E.S. and Pace,N.R. (1992) *J. Biol. Chem.*, **267**, 2429–2436.
15. Hardt,W.-D. and Hartmann,R.K. (1996) *J. Mol. Biol.*, **259**, 422–433.
16. Hartmann,R.K. and Erdmann,V.A. (1991) *Nucleic Acids Res.*, **19**, 5957–5964.
17. Vogel,D.W., Hartmann,R.K., Kröger,B., Ulbrich,N. and Erdmann,V.A. (1987) *Biochem. Int.*, **14**, 167–175.
18. Rivera-León,R., Green,C.J. and Vold,B.S. (1995) *J. Bacteriol*., **177**, 2564–2566.
19. Heide,C., Pfeiffer,T., Nolan,J.M. and Hartmann,R.K. (1999) *RNA*, **5**, 102–116.
20. Warnecke,J.M., Held,R., Busch,S. and Hartmann,R.K. (1999) *J. Mol. Biol.*, **290**, 433–445.
21. Beebe,J.A. and Fierke,C.A. (1994) *Biochemistry*, **33**, 10294–10304.
22. Cosstick,R. and Vyle,J.S. (1990) *Nucleic Acids Res.*, **18**, 829–835.
23. Weinstein,L.B., Earnshaw,D.J., Cosstick,R. and Cech,T.R. (1996) *J. Am. Chem. Soc.*, **118**, 10341–10350.
24. Brännvall,M. and Kirsebom,L.A. (1999) *J. Mol. Biol.*, **292**, 53–63.
25. Krupp,G., Kahle,D., Vogt,T. and Char,S. (1991) *J. Mol. Biol.*, **217**, 637–648.
26. Crary,S.M., Niranjanakumari,S. and Fierke,C.A. (1998) *Biochemistry*, **37**, 9409–9416.
27. Pan,T. and Zhong,K. (1994) *Biochemistry*, **33**, 14207–14212.
28. Frey,P.A. and Sammons,R.D. (1985) *Science*, **228**, 541–545.
29. Pecoraro,V.L., Hermes,J.D. and Cleland,W.W. (1984) *Biochemistry*, **23**, 5262–5271.
30. Sigel,R.K.O., Song,B. and Sigel,H. (1997) *J. Am. Chem. Soc.*, **119**, 744–755.
31. Brautigam,C.A., Sun,S., Piccirilli,J.A. and Steitz,T.A. (1999) *Biochemistry*, **38**, 696–704.
32. Warnecke,J.M., Green,C.J. and Hartmann,R.K. (1997) *Nucl. Nucl.*, **16**, 721–725.
33. Loria,A. and Pan,T. (1998) *Biochemistry*, **37**, 10126–10133.
34. Brautigam,C.A. and Steitz,T.A. (1998) *J. Mol. Biol.*, **277**, 363–377.
35. Curley,J.F., Joyce,C.M. and Piccirilli,J.A. (1997) *J. Am. Chem. Soc.*, **119**, 12691–12692.
36. Podar,M., Perlman,P.S. and Padgett,R.A. (1995) *Mol. Cell. Biol.*, **15**, 4466–4478.
37. Podar,M., Perlman,P.S. and Padgett,R.A. (1998) *RNA*, **4**, 890–900.